

ESD-TR-67-321  
ESTI FILE COPY

ESD RECORD COPY

RETURN TO  
SCIENTIFIC & TECHNICAL INFORMATION DIVISION  
(ESTI), BUILDING 1211

ESD ACCESSION LIST

ESTI Call No. **1 AL 57549**

Copy No.        of        cys.

Technical Note

1967-29

Earth Coverage  
from a Circularly Symmetric  
Shaped-Beam Antenna  
on a Synchronous Satellite

J. B. Rankin

27 June 1967

Prepared under Electronic Systems Division Contract AF 19(628)-5167 by

**Lincoln Laboratory**

MASSACHUSETTS INSTITUTE OF TECHNOLOGY

Lexington, Massachusetts



AD0656707

The work reported in this document was performed at Lincoln Laboratory, a center for research operated by Massachusetts Institute of Technology, with the support of the U.S. Air Force under Contract AF 19(628)-5167.

This report may be reproduced to satisfy needs of U.S. Government agencies.

This document has been approved for public release and sale; its distribution is unlimited.

MASSACHUSETTS INSTITUTE OF TECHNOLOGY  
LINCOLN LABORATORY

EARTH COVERAGE FROM A CIRCULARLY SYMMETRIC  
SHAPED-BEAM ANTENNA ON A SYNCHRONOUS SATELLITE

*J. B. RANKIN*

*Group 61*

TECHNICAL NOTE 1967-29

27 JUNE 1967

LEXINGTON

MASSACHUSETTS

## ABSTRACT

Calculations have been made to show the earth illumination from circularly symmetric antennas on synchronous satellites. The antenna directive gain is calculated as a function of antenna size, beam shape, intended beam pointing direction, error in the pointing direction, and the fraction of the earth surface illuminated.

Accepted for the Air Force  
Franklin C. Hudson,  
Chief, Lincoln Laboratory Office

## Earth Coverage From a Circularly Symmetric Shaped-Beam Antenna on a Synchronous Satellite

### INTRODUCTION

In a memorandum entitled "Earth Coverage Patterns with High-Gain Antennas on Stationary Satellites," W. Sollfrey<sup>1</sup> calculates and displays the portion of the earth's surface illuminated by an antenna beam from a stationary, synchronous, equatorial satellite. Parameters are beam size and pointing direction relative to the sub-satellite point. Figure 1 shows such a synchronous satellite at Q with its antenna pointed at point P on earth; in Fig. 1, P is shown due north of the sub-satellite point L. The angular deviation  $\beta$  of P from L measured at the earth center is called the offset angle. The deviation  $\gamma$  measured at the satellite is the beam pointing angle. Sollfrey determined the intersection of right circular cones of apex angle  $2\alpha$  with a sphere as a function of  $\gamma$  (and hence  $\beta$ ) and another angle  $\eta$  which locates P relative to the north-south meridian through L. In Fig. 1,  $\eta = 0$ . The intersection curves are plotted on a Mercator projection of earth latitude and longitude. In each family  $\beta$  and  $\eta$  are constant, and the different curves are for different  $\alpha$ . An overlay projection of the earth to the same scale can be superimposed on these curves to display that portion of the earth illuminated within the different cones. The effect of moving the sub-satellite point along the equator can be seen by sliding the earth map along a plot of the curves. These superimposed charts will then be maps of antenna gain, provided one knows what antenna gain is obtain-

able at and within angle  $\alpha$  measured from the antenna pointing direction.

Sollfrey's memo confines itself to the geometric problem only.

A first object of this technical note is to calculate antenna directive gain\* for circularly symmetric beams at different angles  $\alpha$  as a function of antenna size and beam shape. The results are presented as curves. There are three families of curves, one family for each of three beam shapes. The curves are plotted as antenna directive gain in fixed direction  $\alpha$  vs antenna size (actually a parameter related to size). The different members of each family are for different  $\alpha$ . The equations used for calculating these curves are also used for calculating principal plane antenna patterns. There are three families of patterns, one family for each of the three beam shapes. The different patterns in a family are for different size antennas.

A second object is to calculate the earth area enclosed within cones of different  $\alpha$ . The results are a family of curves in which the parameter is the offset angle  $\beta$ . The abscissa scale is this area  $S$  normalized with respect to the maximum usable earth area, which is that portion of the earth's surface  $S_{\Delta}$  from which the satellite is seen at an elevation angle greater than  $\Delta$ . This is shown in Fig. 2. Rather than cone angle  $\alpha$ , antenna directive gain is used as the ordinate — that is, the maximum directive gain which can be obtained in direction  $\alpha$  from proper choice of the size of a uniformly illuminated circular

---

\*Antenna directive gain rather than absolute gain is calculated, because it is the directive gain that is a function of the antenna pattern.

aperture. Assaly<sup>2</sup> showed that this directive gain is  $(1.16373/\sin\alpha)^2$ , where 1.16373 is twice the maximum value of  $J_1(x)$ .

#### ANTENNA DIRECTIVE GAIN AT ANGLE $\alpha$ OFF BEAM POINTING DIRECTION

Figures 3a, b, and c are principal plane antenna directive gain patterns for circularly symmetric antenna beams. Each figure is for a single pattern shape and hence a single circularly symmetric aperture distribution as a function of normalized radius. Let  $g(u)$ ,  $u = \frac{\pi D}{\lambda} \sin\alpha$ , denote the field pattern shape (but not the gain) and  $f(r)$ ,  $0 \leq r \leq 1$ , denote the aperture distribution. Let  $G(\alpha)$  denote the directive gain in direction  $\alpha$ . The different curves in any one figure are for different size apertures. A single curve is  $G(\alpha)$  in db vs  $\alpha$ , where  $\alpha$  is plotted in a logarithmic scale.  $D/\lambda$  is the aperture diameter in wavelengths.

Figure 3a is for a uniformly illuminated circular aperture.

$$g(u) = \frac{2J_1(u)}{u} ; \text{ in this form } g(0) = 1 \quad (1)$$

$$G(\alpha) = \left\{ \frac{2J_1\left(\frac{\pi D}{\lambda} \sin\alpha\right)}{\sin\alpha} \right\}^2 \quad (2)$$

The reason for plotting  $\alpha$  on a logarithmic scale is that for small  $\alpha$ ,  $\sin\alpha \approx \alpha$ , where  $\alpha$  is in radians; hence the patterns all look alike.

Figures 3b and c are for shaped beams. The shaping is obtained by using two and four terms respectively according to John Ruze's Bessel function



### "Circular Aperture Synthesis." <sup>3</sup>

The general expression for  $g(u)$  is

$$g(u) = 2 \sum_{j=0}^N \frac{g(\beta_j)}{J_0(\beta_j)} \times \frac{u J_1(u)}{u^2 - \beta_j^2} \quad (3)$$

where  $\beta_j$  are the zeros of  $J_1(u)$  and  $g(\beta_j)$  are the coefficients of the terms.  $\beta_j$  should not be confused with angle  $\beta$  in Fig. 1.  $g(\beta_j)$  can be complex:  $A_j \exp(i\psi_j)$ .

The following values were used:

For Figure 3b		
j	0	1
$A_j$	1	1
$\psi_j$	0	45°

For Figure 3c				
j	0	1	2	3
$A_j$	1	1	1	0.97
$\psi_j$	0	0	0	45°

Note that the uniformly illuminated circular aperture can be called a single-term Ruze synthesis ( $A_0 = 1$ ;  $\psi_0 = 0$ ).

The three beam shapes for  $|g(u)|^2$  are plotted in Fig. 4. Also shown on Fig. 4 are the values for  $u_m$ ;  $u_m$  will be defined later. The Ruze procedure could also be used to synthesize full-earth coverage shaped beams as described by King, Wong, and Zamites<sup>4</sup> in which the beam shape is tailored to compensate for propagation effects, including distance.

Ruze gives the formula for the on-axis directivity:



$$G(0) = \left(\frac{\pi D}{\lambda}\right)^2 \frac{|g(0)|^2}{\sum_{j=0}^N \frac{|g(\beta_j)|^2}{J_o^2(\beta_j)}} \quad (4)$$

where the absolute value signs have been added to allow for complex  $g(\beta_j)$ . The directivity in any direction  $\alpha$ ,  $G(\alpha)$ , is

$$G(\alpha) = G(0) \frac{|g(u)|^2}{|g(0)|^2}; u = \frac{\pi D}{\lambda} \sin \alpha \quad (5)$$

$$G(\alpha) = \left(\frac{\pi D}{\lambda}\right)^2 \frac{1}{\sum_{j=0}^N \frac{|g(\beta_j)|^2}{J_o^2(\beta_j)}} \cdot |g(u)|^2; u = \frac{\pi D}{\lambda} \sin \alpha \quad (6a)^*$$

$$G(\alpha) = \left(\frac{\pi D}{\lambda}\right)^2 \frac{4 \left| \sum_{j=0}^N \frac{g(\beta_j)}{J_o(\beta_j)} \times \frac{u J_1(u)}{u^2 - \beta_j^2} \right|^2}{\sum_{j=0}^N \frac{|g(\beta_j)|^2}{J_o^2(\beta_j)}}; u = \frac{\pi D}{\lambda} \sin \alpha \quad (6b)$$

The curves of Figs. 3b and c are calculated from Eq. (6b). As was the case for Fig. 3a, the curves of Fig. 3b all look alike; likewise those of Fig. 3c.

---

\* Eq. (6a) for  $G(\alpha)$  is introduced here for use in Appendix I.

The reason for using Ruze's "Circular Aperture Synthesis" to calculate the patterns for this note is that it provides an expeditious means for generating patterns of a desired shape and beamwidth. Antenna directive gain in any direction is included. The method tells what aperture size and distribution are needed to produce the combination of pattern shape and beamwidth. Presumably there exist other aperture distributions for essentially the same amplitude pattern, but a smaller size antenna would imply supergain.

For each set of curves in Fig. 3, a dotted line is drawn tangent to the "knees" of the curves. The effect of increasing the antenna diameter is to displace the pattern up and to the left; decreasing the size, down and to the right. The dotted line is the maximum directive gain obtainable in direction  $\alpha$  for a pattern of the given shape. In order to realize this maximum directive gain in some particular direction  $\alpha_m$ , one must choose the proper antenna size. Antennas which are larger, as well as those which are smaller, will have less gain in direction  $\alpha_m$ .  $\alpha_m$  is the parameter for the different curves on each figure.

So far no allowance has been made for error in the pointing direction of the satellite antenna. Suppose the error is  $\delta$  degrees. Then if the curves of Fig. 3 say that a certain directive gain is obtainable in direction  $\alpha$ , this gain can be expected 100% of the time only for angle  $\alpha - \delta$  because of the pointing error\*. Since  $\alpha$  is plotted on a logarithmic scale, the correction must be

---

\* Correction on a probabilistic basis is more complicated and will not be made here.

made numerically, rather than by graphically displacing the curves.

Comparison of Figs. 3a, b, and c shows that the two-term Bessel shaped beam of Fig. 3b can achieve 2 db more directivity in any direction  $\alpha$  than can the uniformly illuminated aperture. The four-term Bessel shaped beam can achieve an additional 1.4 db. However, realization of the improvement requires proper choice of antenna size.

Figures 5a, b, and c show the data of Figs. 3a, b, and c, respectively in a different way — that is, they show more directly  $G(\alpha)$  in certain fixed directions  $\alpha$  as a function of antenna design. As before the ordinate is directivity in db. The abscissa is the angle  $\alpha_m$  mentioned above, that is, the angle for which the antenna size was chosen in order to maximize the directive gain in that direction. In any one figure, the different curves are for different values of  $\alpha$ . The three different figures are for the three different pattern shapes already described.

Expressions for the curves are developed as follows. If one knows the pattern shape  $g(u)$  vs  $u$ , where  $u = (\pi D/\lambda) \sin \alpha$ , one can calculate the size  $\pi D/\lambda$  which maximizes the directivity in any direction  $\alpha_m$  without resort to families of curves such as Fig. 3. First one finds a value  $u_m$  which is a solution to the differential equation:

$$u \frac{d}{du} |g(u)|^2 + 2 |g(u)|^2 = 0 \quad . \quad (7)$$

The above form allows for the possibility that  $g(u)$  be complex. If  $g(u)$  is real,

it may be simpler to use:

$$u \frac{d}{du} g(u) + g(u) = 0 \quad . \quad (8)$$

Then the diameter  $D_m$  is given by:

$$\frac{D_m}{\lambda} = \frac{u_m}{\pi \sin \alpha_m} \quad . \quad (9)$$

Derivation of Eq. (7) will be given in Appendix I.

For plotting Fig. 5, the directive gain pattern, Eq. (6), can be rewritten to show explicitly the dependence of  $G(\alpha)$  on  $\alpha_m$  by substituting Eq. (9) into Eq. (6):

$$G(\alpha, \alpha_m)^* = \left( \frac{u_m}{\sin \alpha_m} \right)^2 \frac{4 \left| \sum_{j=0}^N \frac{g(\beta_j)}{J_0(\beta_j)} \times \frac{\frac{u_m \sin \alpha}{\sin \alpha_m} J_1 \left( \frac{u_m \sin \alpha}{\sin \alpha_m} \right)}{\left( \frac{u_m \sin \alpha}{\sin \alpha_m} \right)^2 - \beta_j^2} \right|^2}{\sum_{j=0}^N \frac{|g(\beta_j)|^2}{J_0^2(\beta_j)}} \quad . \quad (10)$$

Each curve in Fig. 5 is a plot of  $G(\alpha, \alpha_m)$  vs  $\alpha_m$  for fixed  $\alpha$ . For any one family of curves (7a, b, or c)  $u_m$  has a single value; these values were shown on Fig. 4 and are listed here:

---

\*  $G(\alpha, \alpha_m)$  means the directivity in direction  $\alpha$  when the antenna size is chosen to maximize the directivity in direction  $\alpha_m$ .

<u>Figure</u>	<u>Pattern Name</u>	<u>N</u>	<u><math>u_m^*</math></u>
5a	Uniform Illumination	0	1.85
5b	Two-Term Bessel	1	4.20
5c	Four-Term Bessel	3	9.90

By definition, each curve of  $G(\alpha, \alpha_m)$  vs  $\alpha_m$  is a maximum when  $\alpha_m = \alpha$ . As was the case with Fig. 3, all the curves of any one family look alike. For each family of curves, the locus of maxima,  $G(\alpha_m = \alpha)$  vs  $\alpha_m$ , is the same curve as the tangent curve in Fig. 3a, b, or c. Since  $\alpha$  and  $\alpha_m$  were limited to values such that  $\sin \alpha_m \approx \alpha_m$ , the tangent curve and locus of maxima are very nearly straight lines on the coordinate scales chosen. The size required to maximize the gain in direction  $\alpha_m$  by each of the three pattern shapes is shown on log-log paper in Fig. 4. Each curve is a plot of  $\pi D_m / \lambda$  vs  $\alpha_m$ .

Correction for a beam pointing error of  $\delta$  is made as follows. The directive gains calculated for directions  $\alpha$  from the intended pointing direction can be expected 100% of the time only for directions  $\alpha - \delta$ . One can simply re-label the curves, replacing angle  $\alpha$  by  $\alpha - \delta$ .

The results of the calculations of directivity  $G(\alpha, \alpha_m)$  vs  $\alpha_m$  will now be discussed, starting with those for the uniformly illuminated circular aperture, Fig. 5a. Consider the directive gain at  $\alpha = 4^\circ$ . This corresponds to Sollfrey's

---

\* The values for  $u_m$  are to the nearest 0.05. For uniform illumination,  $u_m$  is readily found analytically to be 1.8412.

8° contour. The maximum directive gain is 24.45 db and is obtained when  $\alpha_m = 4^\circ$  and  $D_m/\lambda = 8.40$ . The gain at  $\alpha = 4^\circ$  is within half a db of the maximum over the range  $3.3^\circ \leq \alpha_m \leq 5.1^\circ$ . One might say that near  $\alpha_m = \alpha$ , the gain  $G(\alpha)$  is not a very critical function of  $\alpha_m$ .

In Fig. 5b the maximum directive gain at  $4^\circ$  is 26.45 db, 2 db higher than for the uniformly illuminated aperture. All corresponding peaks are 2 db higher. The same conclusion was shown by comparison of the tangent lines in Figs. 3a and b. For  $\alpha_m = 4^\circ$ ,  $D_m/\lambda = 19.17$ . For  $\alpha = 4^\circ$  the directive gain is within half a db of the maximum over the range  $3.5^\circ \leq \alpha_m \leq 4.6^\circ$ , which is a smaller range than for the uniformly illuminated aperture. One knows from the pattern shape that  $G(\alpha, \alpha_m)$  is a more critical function of  $\alpha_m$ ; these curves show how much. However, the gain obtainable at  $\alpha = 4^\circ$  for the shaped beam exceeds the maximum (at  $\alpha = 4^\circ$ ) from the uniformly illuminated aperture for  $3.2^\circ \leq \alpha_m \leq 5.7^\circ$ .

In Fig. 5c the maximum directive gain at  $\alpha = 4^\circ$  is 27.9 db, another 1.4 db increase. For  $\alpha_m = 4^\circ$ ,  $D_m/\lambda = 45.18$ . The gain at  $\alpha = 4^\circ$  for this four-term shaped beam exceeds the maximum obtainable from the uniformly illuminated aperture for  $3.45^\circ \leq \alpha_m \leq 5.75^\circ$ .

So far the shaped beams would appear to offer more directive gain than the simple beams. In application, one may be limited by antenna size, and the design question becomes one of the best use of antenna size. This is a complex question involving much more than antenna design; the question cannot

be answered here. What is shown in Figs. 7a, b, and c is comparisons of the three different shape patterns when produced by the same size antenna. Each figure has three curves of  $G(\alpha)$  in db vs  $\alpha$ , where this time  $\alpha$  is plotted on a linear scale. The three curves are for the three different pattern shapes already used. On any one figure the three curves are for the same size antenna. The size is shown as the diameter in wavelengths; values are 10 for Fig. 7a, 16 for Fig. 7b, and 25 for Fig. 7c.

To summarize this section, the antenna directive gain has been calculated as a function of the three variables: (a) angle off boresight, (b) antenna size, and (c) pattern shape. The results are shown in Figs. 3, 5, and 7, each of which has three families of curves (Figs. 3a, b, and c, etc.). In all cases the ordinate scale is antenna directive gain in db. A table of figure numbers, the abscissa scale, the variable parameter distinguishing among the curves of one family, and the parameter distinguishing among the families is as follows:



<u>Figure Numbers</u>	<u>Abscissa Scale</u>	<u>Parameter which identifies the curves on one figure</u>	<u>Parameter(s) which distinguish among the figures of a set</u>
3 a, b, c,	Angle off boresight	Angle for which directive gain is maximized through choice of antenna size	Pattern shape
5 a, b, c,	Angle for which directive gain is maximized through choice of antenna size	Angle off boresight at which directivity is calculated	Pattern shape
7 a, b, c	Angle off boresight	Pattern shape	Antenna size $D/\lambda$

#### ANTENNA DIRECTIVE GAIN VS ILLUMINATED EARTH AREA

The antenna directive gain vs the illuminated earth area is shown by the curves of Fig. 8. The gain  $G(\alpha)$ , is that at angle  $\alpha$  measured from the pointing direction, and the earth area is that contained within a cone defined by  $\alpha$ , as shown in Fig. 2. The results are a family of curves in which the parameter is the offset angle  $\theta_y$  of point P toward which the beam is aimed.  $\theta_y$  is measured from the earth-satellite radial. The offset angle is  $\beta$  in Sollfrey's Fig. 1.

The abscissa scale in Fig. 8 is the earth area  $S$  normalized with respect to the maximum usable earth area  $S_\Delta$ .  $S_\Delta$  is that portion of the earth's surface from which the satellite can be seen at an elevation angle greater than  $\Delta$ . For the Fig. 8 curves,  $\Delta = 10^\circ$ . In some cases the antenna beam extends beyond  $S_\Delta$ . Area  $S$  is defined as being within cone  $\alpha$  and within  $S_\Delta$ . The normalized area is plotted on a logarithmic scale in percent.

The ordinate scale is the directive gain  $G(\alpha_m = \alpha)$  in db. That is, at each angle  $\alpha$ , the value used for  $G(\alpha)$  is the maximum gain obtainable from a pattern of particular shape through proper choice of its size. The pattern shape is  $2J_1(u)/u$ , that of a uniformly illuminated circular aperture. For this shape:  $G(\alpha_m = \alpha) = (1.16373/\sin\alpha)^2$ , where 1.16373 is twice the maximum value of  $J_1(u)$ .  $G(\alpha_m = \alpha)$  vs  $\alpha$  is the tangent curve of Fig. 3a and is also the locus of maxima in Fig. 5a.

The results of Fig. 8 can be extended to pattern shapes other than the  $2J_1(u)/u$  produced by a uniformly illuminated circular aperture. The information used from the pattern is  $G(\alpha_m = \alpha)$  vs  $\alpha$ . For the two-term Bessel pattern used in Figs. 3b and 5b it was found that  $G(\alpha_m = \alpha)$  was 2 db more than for the uniformly illuminated circular aperture, and this is true for all values of  $\alpha$ . The 2 db is the difference between the loci of maxima in Figs. 5a and b. The four-term Bessel pattern used for Figs. 3c and 5c offers an additional 1.4 db improvement in  $G(\alpha_m = \alpha)$  vs  $\alpha$  or 3.4 db more than the uniformly illuminated circular aperture.

The correction to the directive gain which can be expected 100% of the time is shown by Fig. 9 for a  $1^\circ$  beam pointing error. Correction is based on the fact that in order to illuminate an area contained within angle  $\alpha$  of the desired pointing direction 100% of the time, the beam must be enlarged to illuminate an area contained within angle  $\alpha + 1^\circ$ . The larger beam of course has less gain, and the correction is shown as a loss in db.

Let us look at the directivity vs area coverage curves, Fig. 8. Start with a beam looking straight down,  $\theta_y = 0$ . For directivities greater than 25 db, the curve of db on a linear scale vs area on a logarithmic scale is nearly a straight line. But then as the beam gets wider, the area increases "faster" than the directivity decreases, because of the curvature of the earth. Now look at the curve for  $\theta_y = 30^\circ$ . Several differences can be seen: (1) at the higher gains, the beam for  $\theta_y = 30^\circ$  covers more area than the beam pointed straight down, (2) the curvature effect shows up for smaller beam sizes, and (3) the curve has a knee where the area contained within cone  $\alpha$  extends beyond  $S_\Delta$ .

The formulas for calculating the curves of Fig. 8 are given in Appendix II.

## CONCLUSIONS

In conclusion, calculations have been made to show the earth illumination from circularly symmetric antennas on synchronous satellites. Factors included are antenna size, beam shape, intended beam pointing direction, error in the pointing direction, and the fraction of the earth surface illuminated. Blanket answers as to what size antenna and what pattern shape are most desirable are beyond the scope of this note. However, one can expect that there will be many applications where full earth coverage with a shaped-beam antenna is desirable. The proper amount of beam shaping is probably equivalent to at least the two-term Bessel pattern, on account of the 2 db gain

improvement over a simple pencil beam, and not more than the four-term Bessel pattern, on account of the accompanying increase in antenna size.

The directive gains for these two cases are  $19\frac{1}{2}$  db and 21 db, respectively.

## APPENDIX I

### Determination of Antenna Size for Given Shape Pattern $g(u)$ to Maximize the Gain in a Given Direction Off-Axis

The expression for the gain in any direction  $\alpha$  for a circularly symmetric aperture excitation is given by Eq. (6a).

$$G(\alpha) = \left(\frac{\pi D}{\lambda}\right)^2 \cdot \frac{1}{\sum_{j=0}^N \frac{|g(\beta_j)|^2}{J_o^2(\beta_j)}} \cdot |g(u)|^2; u = \frac{\pi D}{\lambda} \sin \alpha \quad (6a)$$

which can be rewritten:

$$G(\alpha) = G_{\text{unif}}^{(0)} \cdot G_{\text{modif}}^{(0)} \cdot |g(u)|^2; u = \frac{\pi D}{\lambda} \sin \alpha \quad (\text{A-I-1})$$

where  $G_{\text{unif}}^{(0)} = \left(\frac{\pi D}{\lambda}\right)^2$  is the on-axis gain of a uniformly illuminated circular aperture.

$$G_{\text{modif}}^{(0)} = \left[ \sum_{j=0}^N \frac{|g(\beta_j)|^2}{J_o^2(\beta_j)} \right]^{-1} \quad \text{is the on-axis gain modification}$$

factor accompanying the use of additional pattern components.

$|g(u)|^2$  is the power pattern as a function of  $u$  — that is, the power pattern shape.

If  $g(0) = 1$ ,  $|g(u)|^2$  is a power pattern normalized to unity at  $u = 0$ .

Recall that  $\beta_j$  are the zeros of  $J_1(u)$  and that  $g(\beta_j)$  are the coefficients of the terms of the pattern  $g(u)$ . Amplitudes and phases of the coefficients specify the pattern. There is no loss of generality in normalizing the pattern with respect to its value at  $u = 0$  — that is, in setting  $g(0) = 1/0$  — unless one wishes a null at  $u = 0$ .

Given the coefficients  $g(\beta_j)$  and hence the pattern  $g(u)$ , I wish to find the value of  $D/\lambda$  which will maximize  $G(\alpha)$ , the gain in direction  $\alpha$ .

A necessary condition that  $G(\alpha)$  be thus maximized is that  $\frac{\partial}{\partial (\frac{\pi D}{\lambda})} G(\alpha) = 0$ .  
Rewrite Eq. (6a):

$$G(\alpha) = \left(\frac{\pi D}{\lambda}\right)^2 \cdot G_{\text{modif}} \cdot |g(u)|^2; u = \frac{\pi D}{\lambda} \sin \alpha \quad (\text{A-I-2})$$

$G_{\text{modif}}$  is not a function of  $\frac{\pi D}{\lambda}$ . Choice of a particular direction  $\alpha$  means that  $\sin \alpha$  is a constant. We can call the direction  $\alpha_m$ , the direction for which the gain is to be maximized.

$$\begin{aligned} \frac{\partial}{\partial (\frac{\pi D}{\lambda})} G(\alpha) &= G_{\text{modif}} \cdot \left\{ \left(\frac{\pi D}{\lambda}\right)^2 \frac{d}{du} |g(u)|^2 \sin \alpha + |g(u)|^2 2\left(\frac{\pi D}{\lambda}\right) \right\} \\ &= G_{\text{modif}} \cdot \left\{ u \frac{d}{du} |g(u)|^2 + 2 |g(u)|^2 \right\} \end{aligned} \quad (\text{A-I-3})$$

This is to equal zero. Hence a necessary condition for  $G(\alpha)$  to be maximized

through choice of  $\frac{\pi D}{\lambda}$  is that

$$u \frac{d}{du} |g(u)|^2 + 2|g(u)|^2 = 0 \quad (7)$$

or

$$u \frac{d}{du} |g(u)| + |g(u)| = 0 \quad (\text{A-I-4})$$

of if  $g(u)$  is real,

$$u \frac{d}{du} g(u) + g(u) = 0 \quad (8)$$

Equation (7) may be satisfied by more than one value of  $u$ . Let each solution be denoted  $u_q$ . For each value  $u_q$  one can calculate  $\frac{\pi D}{\lambda} = \frac{u_q}{\sin \alpha_m}$  where  $\alpha_m$  is the direction in which the gain is to be maximized. Choice of the desired  $u_q$ , which I shall call  $u_m$ , may require trial of several solutions  $u_q$  together with  $\frac{\pi D}{\lambda}$  in Eq. (6a). The choice may involve additional requirements on the pattern — for instance,  $G(\alpha) \geq G(\alpha_m)$  for  $0 \leq \alpha \leq \alpha_m$ . The simple patterns used here satisfy this condition, and  $u_m$  is the smallest value of  $u$  satisfying Eq. (7).

One might ask the following question about circularly symmetric antennas given any pattern shape  $g(u)$ ,  $u = \frac{\pi D}{\lambda} \sin \alpha$ , for which one wishes to maximize  $G(\alpha)$  through proper choice of  $D/\lambda$ : does Eq. (7) apply? I expect that it does but shall not prove it.



## APPENDIX II

### Formulas Used for Directivity vs % Area

Formulas used for Fig. 8 will now be given. The geometry is shown in Fig. 2 which is the same as Fig. 1 except for labeling the coordinate axes and some additional angles. The key formula is the equation for the boundary of S, which Sollfrey derived in his note. He used earth coordinates, latitude and longitude. A conventional spherical coordinate system would use co-latitude (measured from the North Pole). For calculating S, I prefer spherical coordinates with the origin at the earth center and with the Z axis the radial to the satellite. The X-Z plane is oriented to contain P. Therefore, I made coordinate transformations in Sollfrey's equations to obtain formulas convenient for calculating the curves of Fig. 8.

In order to emphasize certain aspects of the geometry a plan view of half of S is shown in Fig. A. In Fig. A-a, the beam does not enclose the sub-satellite point, nor does it reach to the boundary. In Fig. A-b, it encloses the sub-satellite point and extends beyond the boundary. Of course it can also do either one without the other.

The variable in the calculations is the angle  $\theta$ . The equation for the boundary is  $\phi$  as a function of  $\theta$ . S is then the spherical cap defined by  $\theta_A$  if it exists (the cap exists for  $\alpha > \gamma$ ) plus the integral

$$\int_{\theta_A}^{\theta^*} \phi(\theta) \sin \theta \, d\theta$$

where  $\theta_* = \theta_\Delta$  or  $\theta_B$ , whichever is smaller. The surface is normalized and expressed in percent, as has already been stated.

A step-by-step list of terms used and formulas for calculating them will now be given. Much of this will be a repetition. Included is some of the logic used in the calculation. There are potential pitfalls in that bare formulas yield arguments of Arc sine which exceed one.

1.  $\Delta$  = minimum angle above horizon for which communication is maintained.
2.  $k$  = satellite altitude from earth center measured in earth radii.  
Sollfrey used  $k = 6.6134$  for a synchronous satellite.
3.  $\theta_\Delta = \arccos\left(\frac{1}{k} \cos \Delta\right) - \Delta$ .
4.  $S_\Delta$  = usable earth surface = that portion of earth's surface from which satellite appears at or above angle  $\Delta$ .
5.  $S_\Delta = 2\pi(1 - \cos \theta_\Delta)$ .
6.  $P$  = point on earth surface toward which beam is pointed.
7.  $\theta_\gamma$  = offset angle of  $P$  from sub-satellite point.  $\theta_\gamma$  is an input parameter.
8.  $\gamma$  = pointing direction of antenna beam measured at the satellite.
9.  $\gamma = \arctan\left(\frac{\sin \theta_\gamma}{k - \cos \theta_\gamma}\right)$ .

10.  $\alpha$  = angle which defines the cone  $\alpha = \text{const.}$   $\alpha$  is measured from beam pointing direction.
11.  $\alpha = \text{Arc sin} \left( \frac{1.16373}{\frac{\text{db Directivity}}{20}} \right)_{10}$ . Values for db directivity are input.
12.  $S$  = earth surface within cone  $\alpha$  and within  $S_{\Delta}$ .
13.  $\sigma_S = 100 S/S_{\Delta}$ ;  $S$  will be calculated in step 30 unless step 18 preempts further steps, in which case  $\sigma_S = 100$ .
14.  $2\phi_{\Delta} = \text{Arc length of the boundary of } S_{\Delta} \text{ contained within cone } \alpha$ .
15.  $\sigma_B = \frac{100 \times 2\phi_{\Delta}}{2\pi} = \frac{100\phi_{\Delta}}{\pi}$ ;  $\phi_{\Delta}$  will be calculated in step 26 unless step 18 preempts further steps, in which case  $\sigma_B = 100$ .
16.  $\theta_A$  and  $\theta_B$ , if they exist, are the minimum and maximum  $\theta$  coordinates respectively, measured in the X-Z plane, of the intersection of the cone and the sphere.
17.  $\text{Arg}_A \text{ Arc sin} = k \sin |\gamma - \alpha|$ .
18. If  $k \sin |\gamma - \alpha| > 1$ , then  $\sigma_S = 100$ ,  $\sigma_B = 100$ , and omit steps beyond this one.
19.  $\theta_A = \text{Arc sin} \{k \sin |\gamma - \alpha| - |\gamma - \alpha|\}$ .
20. If  $\theta_A > \theta_{\Delta}$ , then  $\sigma_S = 100$ ,  $\sigma_B = 100$ , and omit steps beyond this one.
21.  $\theta_*$  = upper limit of  $\theta$  for integration.
22.  $\text{Arg}_B \text{ Arc sin} = k \sin (\gamma + \alpha)$ .
23. If  $k \sin (\gamma + \alpha) > 1$ ,  $\theta_* = \theta_{\Delta}$  and omit next two steps.

$$24. \theta_B = \text{Arc sin } \{k \sin (\gamma + \alpha)\} - (\gamma + \alpha).$$

$$25. \theta_* = \text{smaller of } \begin{cases} \theta_\Delta \\ \theta_B \end{cases}.$$

$$26. \phi(\theta) = \text{Arc cos } \left\{ \frac{-(\cos \gamma) (k - \cos \theta) + (\cos \alpha) \sqrt{k^2 - 2k \cos \theta + 1}}{\sin \theta \sin \gamma} \right\}.$$

This is the equation for the intersection of cone  $\alpha$  with the earth sphere. It was obtained from Sollfrey's memorandum by transformation of coordinates.

$$27. \phi_\Delta = \phi(\theta_\Delta) \text{ if } \theta_* = \theta_\Delta$$

$$\phi_\Delta = 0 \quad \text{if } \theta_* = \theta_B.$$

$$28. \text{Integral} = 2 \int_{\theta_A}^{\theta_*} \phi(\theta) \sin \theta \, d\theta.$$

This integral was evaluated by the mid-point rectangular rule, which algebraically is the same as the trapezoidal rule, except that in mid-point rectangular,  $\phi(\theta_A)$  and  $\phi(\theta_*)$  are not used.<sup>‡</sup>

$$29. S_A = \text{the portion of } S \text{ bounded by } \theta = \theta_A.$$

$$30. S_A = \begin{cases} 2\pi(1 - \cos \theta_A) & \text{if } \alpha > \gamma \\ 0 & \text{if } \alpha \leq \gamma \end{cases}.$$

$$31. S = \text{Integral} + S_A.$$

$$32. \text{Calculate } \sigma_S \text{ by step 13, which said } \sigma_S = 100 S/S_\Delta.$$

$$33. \text{Calculate } \sigma_B \text{ by step 15, which said } \sigma_B = 100 \phi_\Delta/\pi.$$

---

<sup>‡</sup> Mid-point rectangular is especially appropriate for integration where the end points are not well behaved. It was used for this problem because it was readily available.

## ACKNOWLEDGMENT

The author wishes to acknowledge that the earth area gain coverage problem was posed by Mr. L. J. Ricardi. All calculations were performed by Mr. Leon Niro on the IBM 7094 and System 360/67 computers.

## REFERENCES

1. W. Sollfrey, "Earth Coverage Patterns with High-Gain Antennas on Stationary Satellites," Rand Memorandum RM-4894-NASA (February 1966).
2. R. N. Assaly, "Probability Distribution of Antenna Gain for Satellite with Switched Antenna System," Technical Report 347, Lincoln Laboratory, M.I.T. (4 February 1964).
3. J. Ruze, "Circular Aperture Synthesis," Trans. IEEE AP-12, No. 6 (November 1964).
4. H.E. King, J.L. Wong and C.J. Zamites, "Shaped Beam Antennas for Satellites," Trans. IEEE AP-14, No. 5 (September 1966).

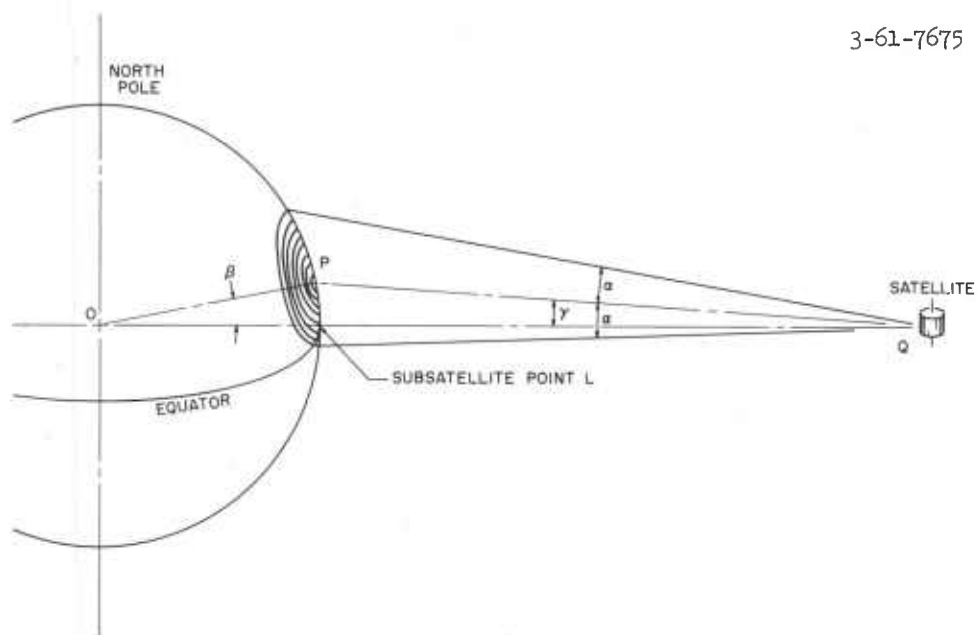


Fig. 1. Antenna beam from satellite illuminating portion of earth surface.



3-61-7673

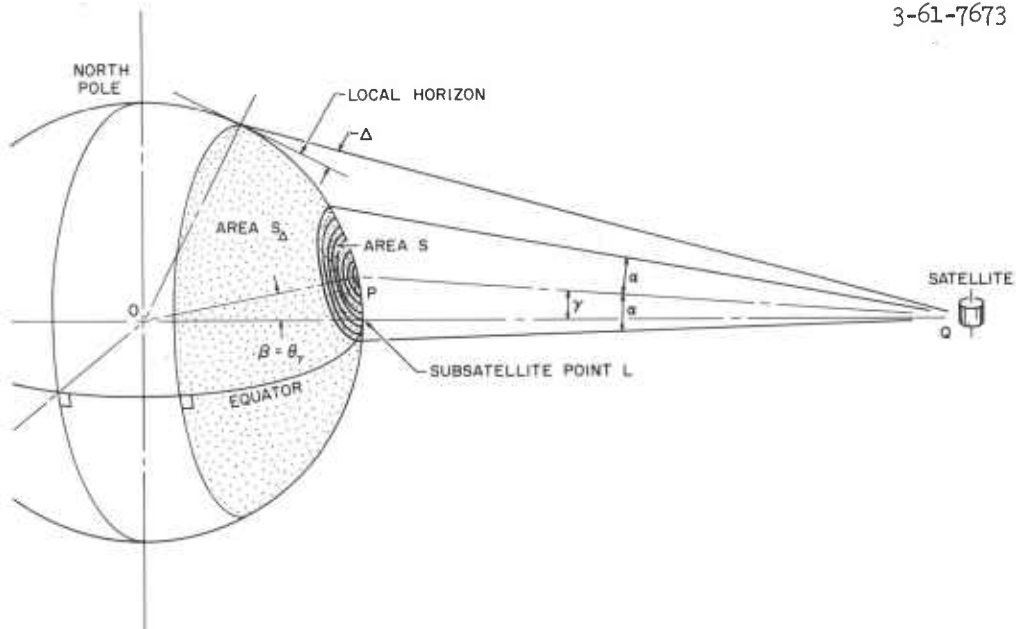


Fig. 2. Antenna beam from satellite illuminating portion of earth surface.

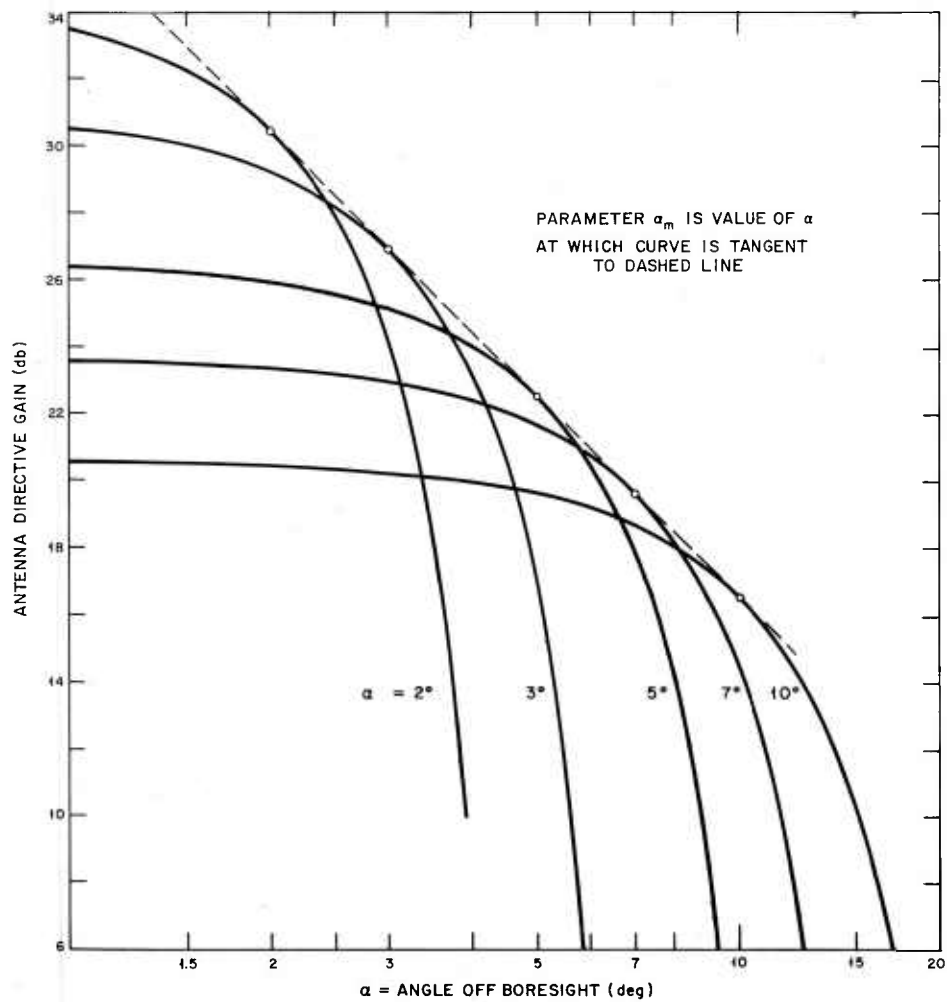


Fig. 3. Directive gain patterns of circular aperture antenna.

a. Pencil beam; uniform aperture distribution.

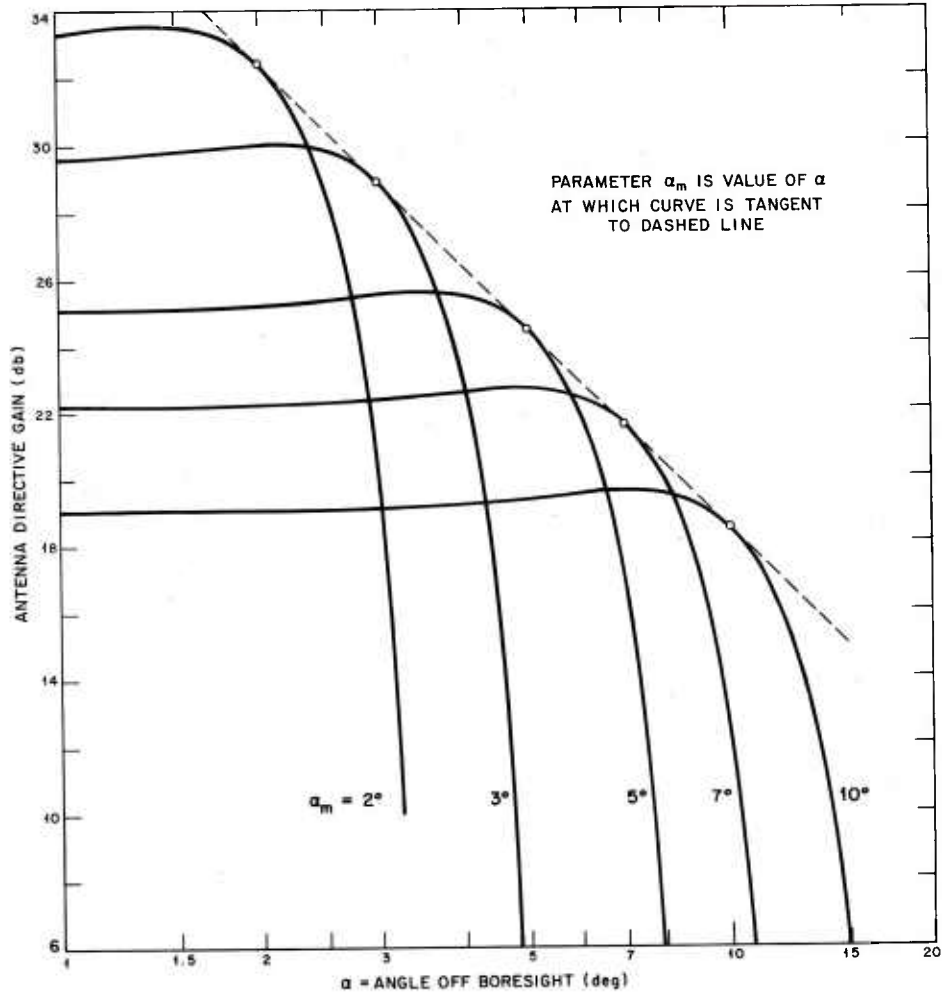


Fig. 3 Con't. b. Flat-top beam; two-term aperture distribution.

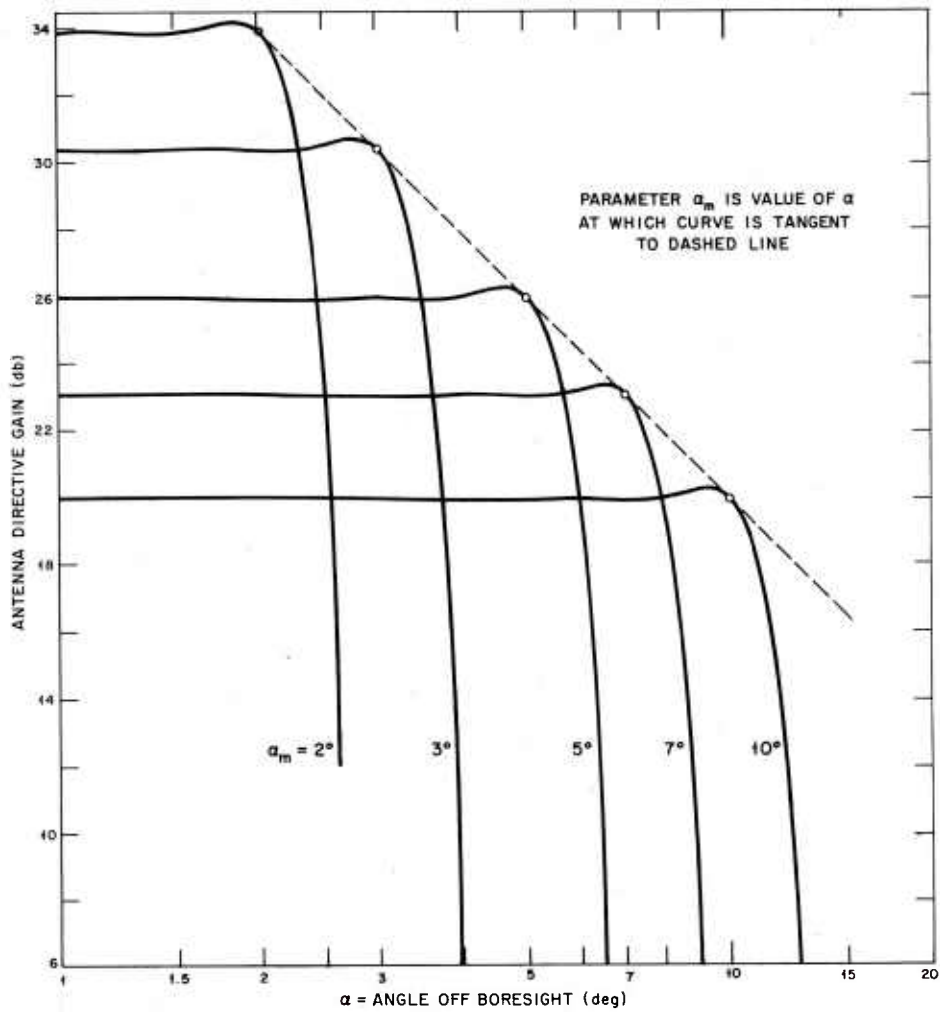


Fig. 3 Con't. c. Flat-top beam; four-term aperture distribution.

3-61-7684

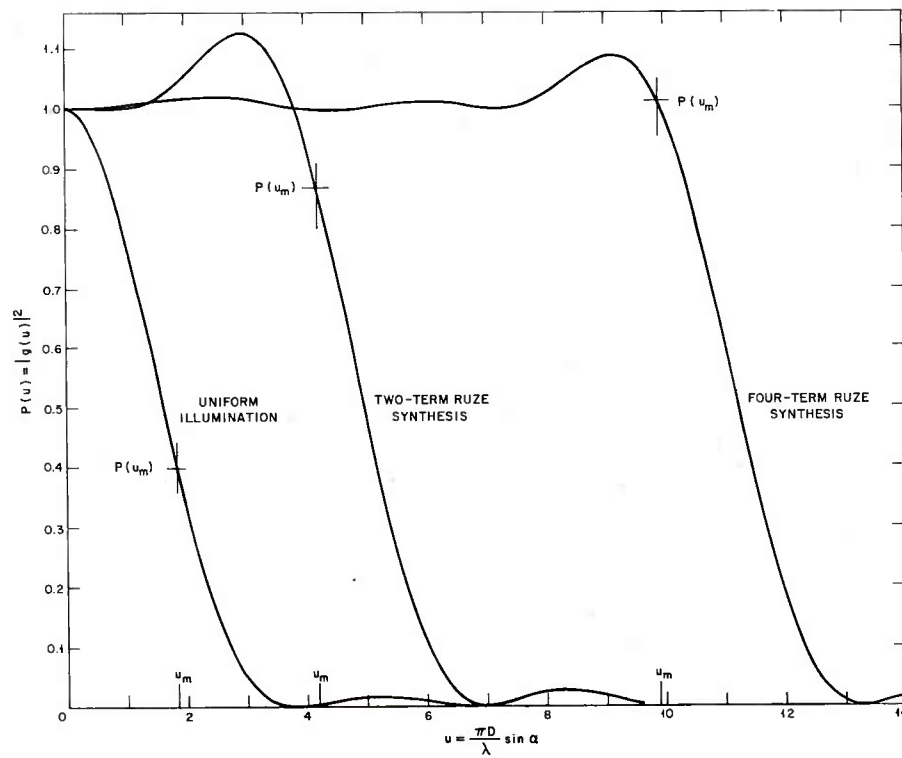


Fig. 4. Normalized power patterns calculated from Ruze's "Circular Aperture Synthesis."

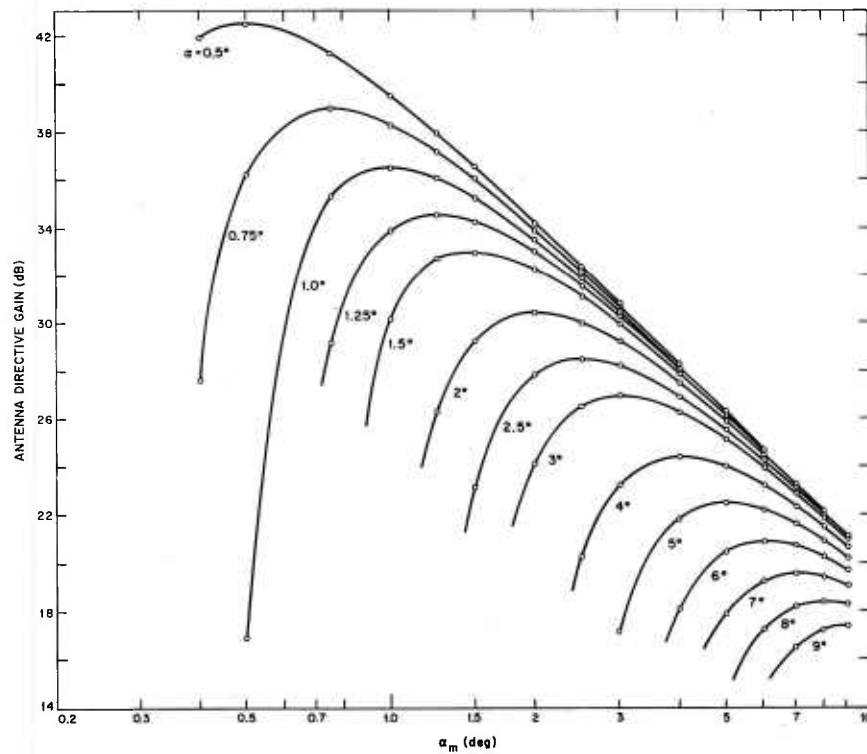


Fig. 5. Directive gain at angle  $\alpha$  vs  $\alpha_m$ .  $\alpha_m$  is the angle for which the gain of a given shape pattern is maximized through proper choice of antenna size.

a. Pencil beam; uniform aperture distribution.

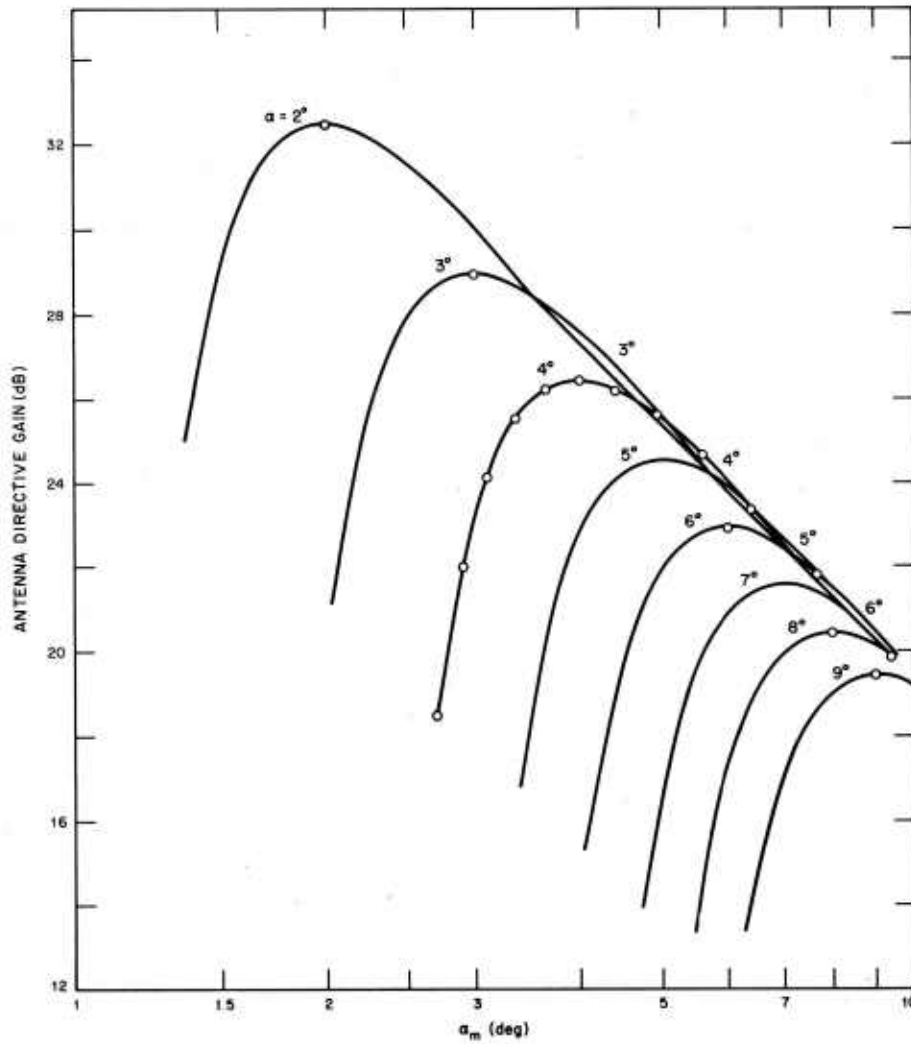


Fig. 5 Con't. b. Flat-top beam; two-term aperture distribution.



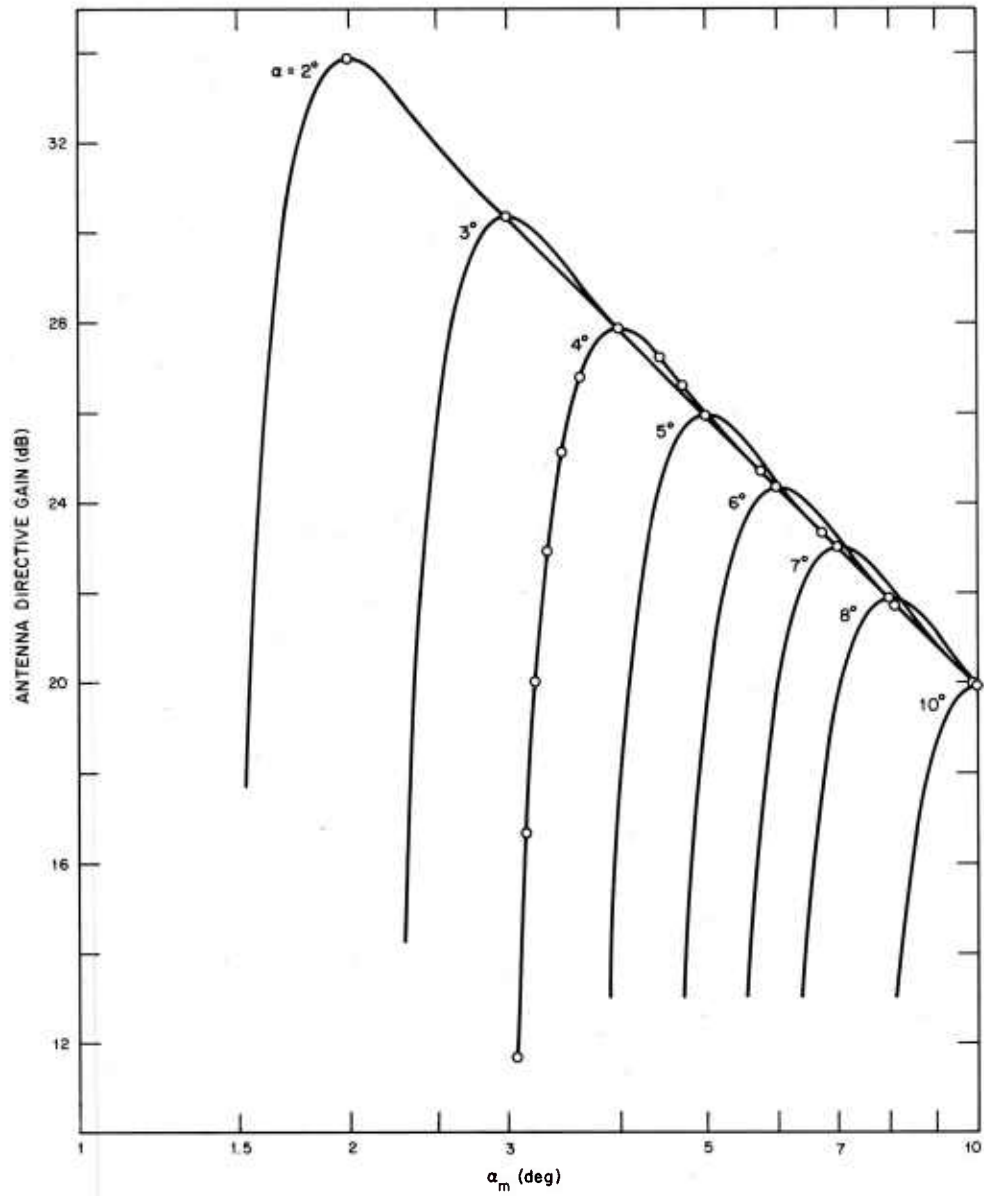


Fig. 5 Con't. c. Flat-top beam; four-term aperture distribution.

3-61-7676

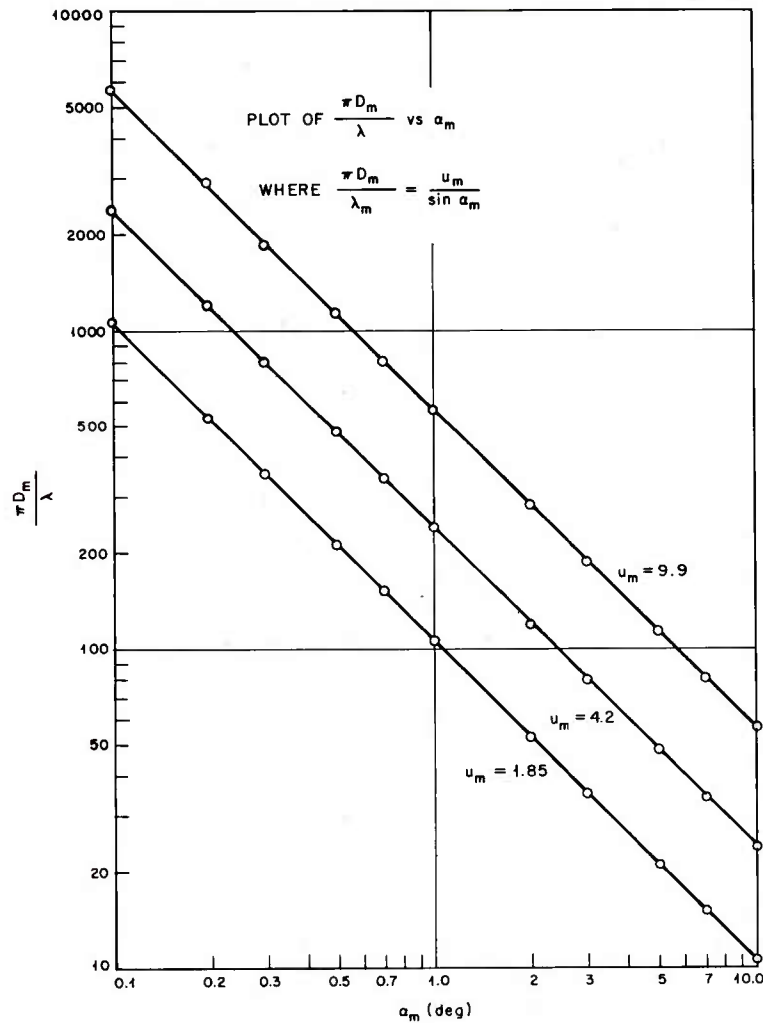


Fig. 6. Antenna size required to maximize the directive gain in direction  $\alpha_m$  for three different pattern shapes.

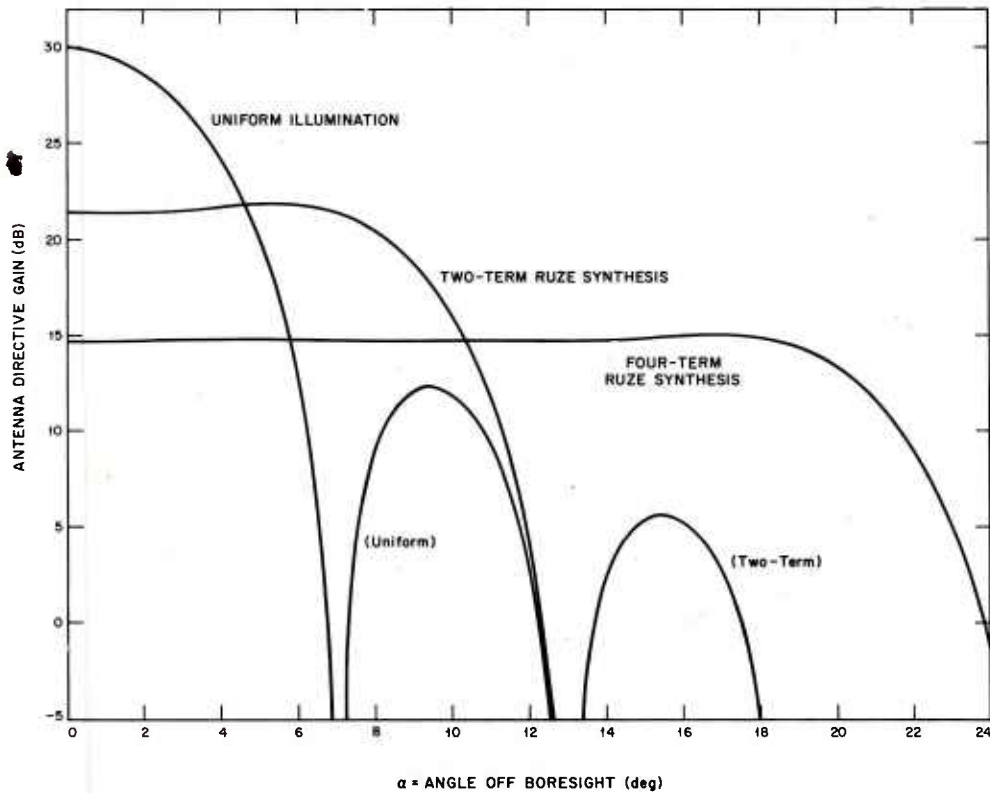
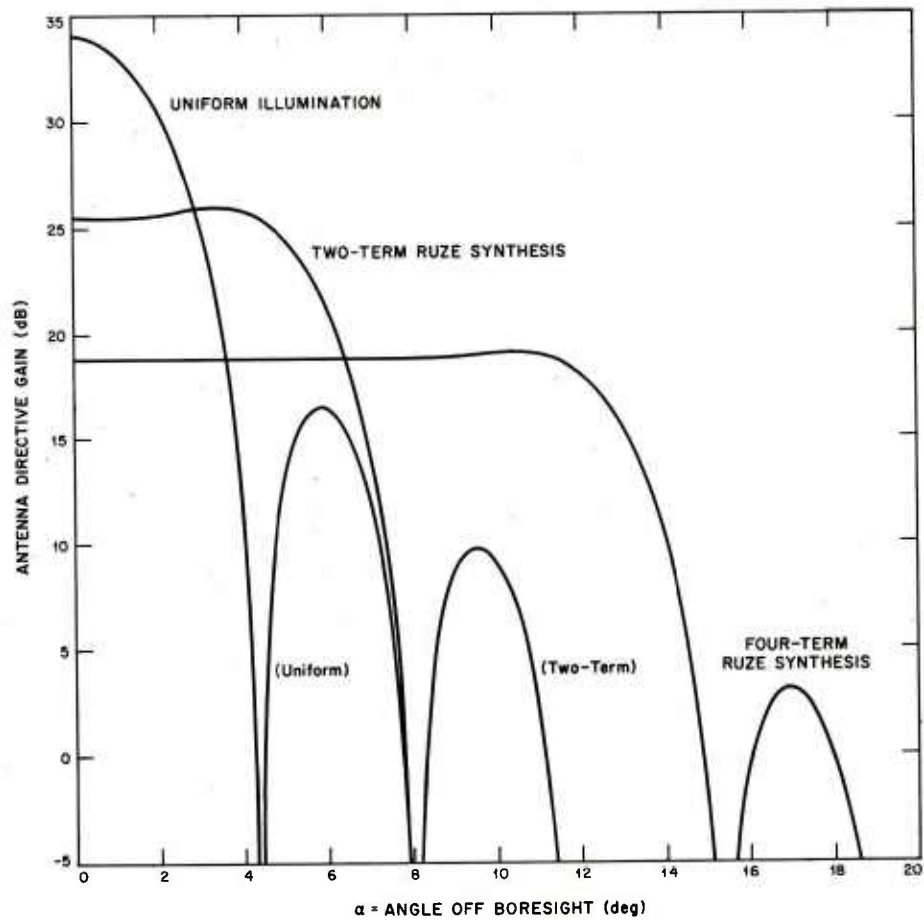
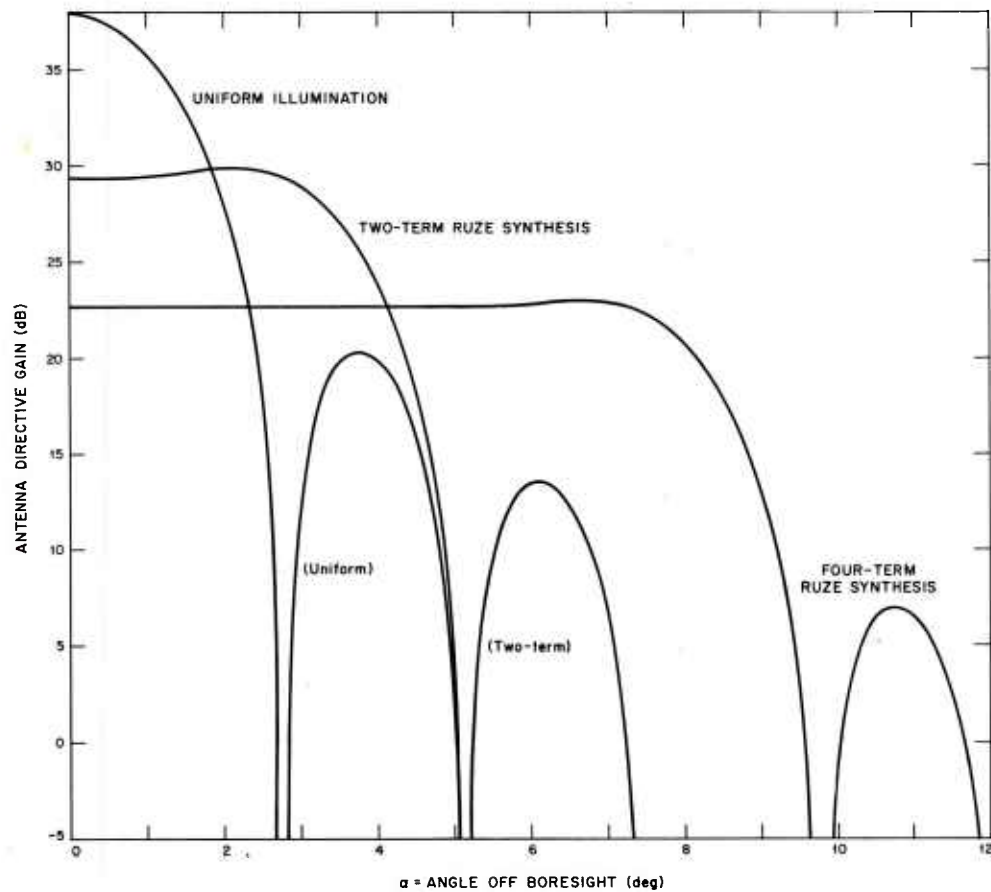


Fig. 7. Directive gain patterns of circular aperture antenna.

a.  $D/\lambda = 10$

Fig. 7 Con't. b.  $D/\lambda = 16$

Fig. 7 Con't. c.  $D/\lambda = 25$

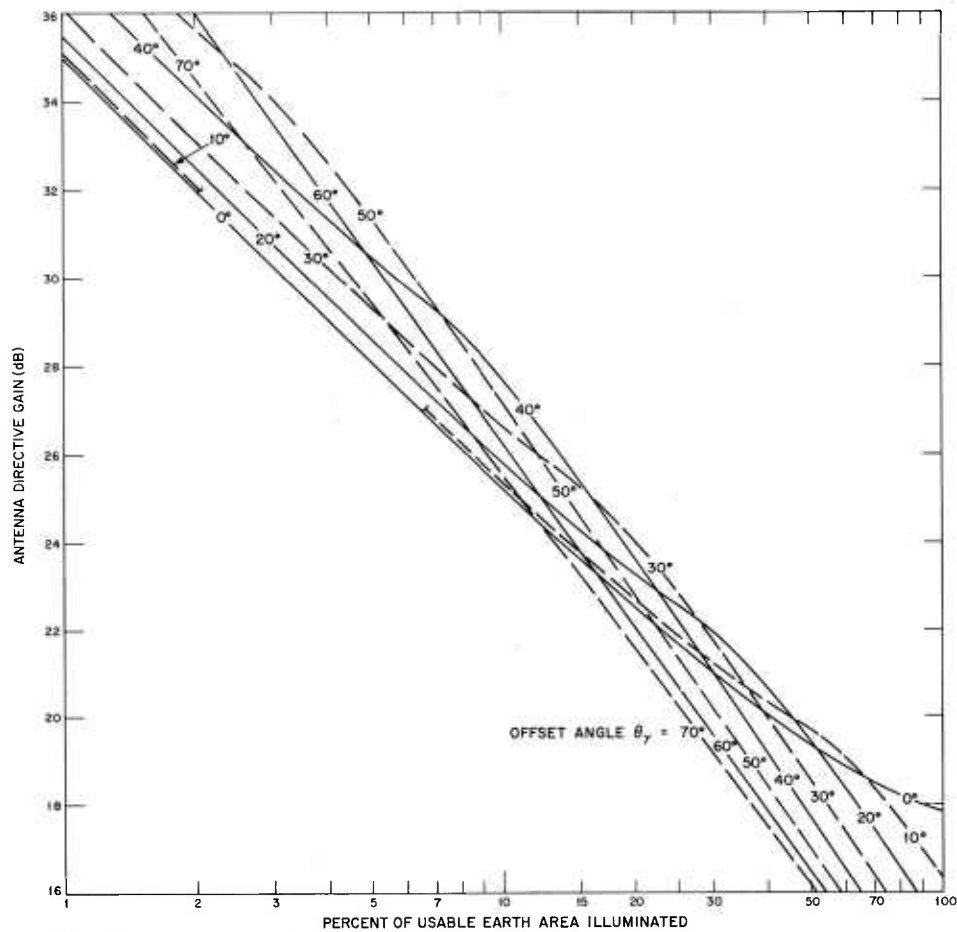


Fig. 8. Antenna directive gain vs earth area illuminated.

Notes: (a) Uniform aperture distribution.

(b) Zero beam pointing error.

(c) For two-term and four-term aperture distributions, increase ordinate scale by 2 db and 3.4 db, respectively.

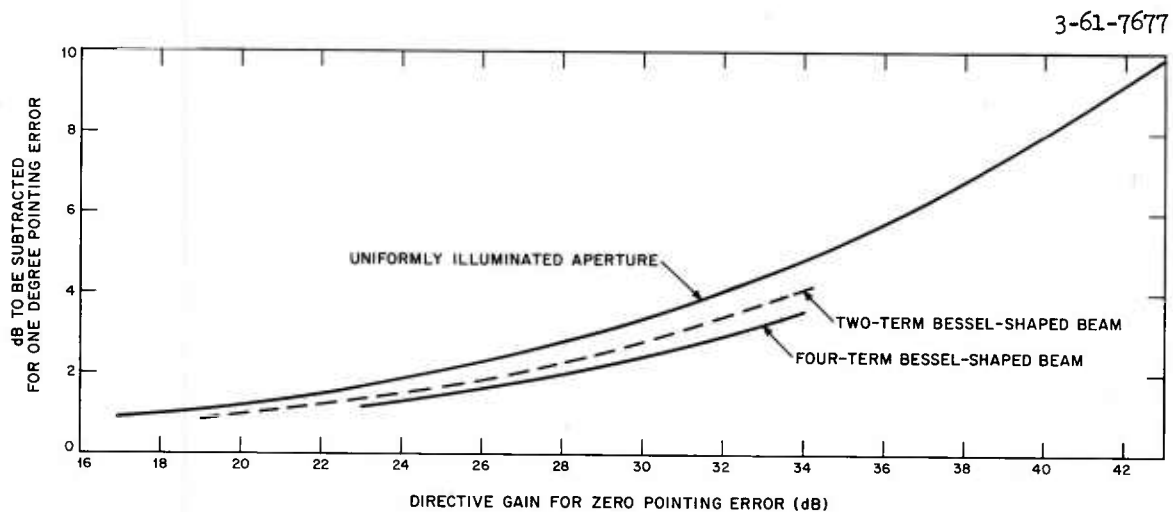
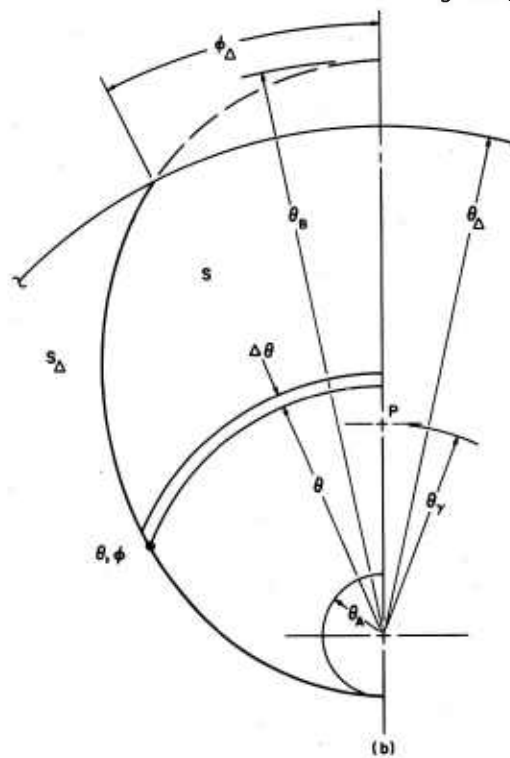


Fig. 9. Corrections to directive gains which can be expected 100% of the time for a  $1^\circ$  beam pointing error. The corrections are applied to the ordinate values of Fig. 8.



- a. S does not enclose subsatellite point.
- b. S encloses subsatellite point.



DOCUMENT CONTROL DATA - R&D		
(Security classification of title, body of abstract and indexing annotation must be entered when the overall report is classified)		
1. ORIGINATING ACTIVITY (Corporate author)  Lincoln Laboratory, M.I.T.		2a. REPORT SECURITY CLASSIFICATION Unclassified
		2b. GROUP None
3. REPORT TITLE  Earth Coverage from a Circularly Symmetric Shaped-Beam Antenna on a Synchronous Satellite		
4. DESCRIPTIVE NOTES (Type of report and inclusive dates) Technical Note		
5. AUTHOR(S) (Last name, first name, initial)  Rankin, J. Bruce		
6. REPORT DATE 27 June 1967	7a. TOTAL NO. OF PAGES 46	7b. NO. OF REFS 4
8a. CONTRACT OR GRANT NO. AF 19 (628)-5167	9a. ORIGINATOR'S REPORT NUMBER(S) Technical Note 1967-29	
b. PROJECT NO.		
c. 649L	9b. OTHER REPORT NO(S) (Any other numbers that may be assigned this report)	
d.	ESD-TR-67-321	
10. AVAILABILITY/LIMITATION NOTICES  This document has been approved for public release and sale; its distribution is unlimited.		
11. SUPPLEMENTARY NOTES  None	12. SPONSORING MILITARY ACTIVITY  Air Force Systems Command, USAF	
13. ABSTRACT  Calculations have been made to show the earth illumination from circularly symmetric antennas on synchronous satellites. The antenna directive gain is calculated as a function of antenna size, beam shape, intended beam pointing direction, error in the pointing direction, and the fraction of the earth surface illuminated.		
14. KEY WORDS  earth coverage synchronous satellite circularly symmetric beams		
circularly symmetric antennas shaped-beam antenna antenna directive gain		